MATHEMATICAL MODEL OF THE WORKING PROCESS OF AN IMPULSE TYPE OF GAS BARRIER FACE SEAL

EDUARD KUZNETSOV[1], ANTON PANDA[2], VOLODYMYR NAHORNYI[1]

[1]Sumy State University, Department of Information Technologies, Faculty of Electronics and Information Technologies, Sumy, Ukraine

[2]Technical University of Kosice, Department of Automotive and Manufacturing Technologies, Faculty of Manufacturing Technologies with a seat in Presov, Slovak Republic

DOI: 10.17973/MMSJ.2025_06_2025024

e-mail: **anton.panda@tuke.sk**

This article provides a mathematical description of the working process of a promising gas seal, which operates with performance characteristics similar to those of the latest gas-dynamic seals but uses a completely different principle of creating the gas barrier, preventing leakage of the pumped product from the pump at the outlet its rotating rotor from the casing. The proposed mathematical dependencies make it possible to calculate the geometric parameters of the sealing rings, which are the main working components of the seal, and to determine the static and dynamic characteristics of the working process in the seal.

KEYWORDS

gas barrier, impulse face seal, flow distribution, dynamic stiffness, transfer function, amplitude frequency characteristics, phase frequency characteristics

1 INTRODUCTION

Until recently, in the chemical industry, liquidic sealing systems were widely used to ensure the prevention of leaks when pumping the product with centrifugal pumps, in which a special liquid neutral to the pumped product was supplied to the gap between the two working face surfaces of the sealing rings. However, leading companies involved in the development and implementation of sealing technology have developed and are widely distributing more promising types of seals – gas seals, which use gas rather than liquid to prevent leakage of the pumped product, which enters into the working gap and ensures non-contact operation of the sealing rings [Martsynkovskyy 2014]. According to their characteristics, these new seals are significantly more economical to operate and use in the industry than liquidic seals [Zaborowski 2007, Kuznetsov 2020, Panda 2021, Sukhodub 2019]. These mainly include seals that use the gas-dynamic principle of creating and maintaining a working gap between face sealing rings moving relative to each other using special spiral grooves several microns deep, which are located on the working face surfaces of these rings [Brunetiere 2024]. The production of such rings with gas dynamic grooves is a very high-tech and, as a result, expensive process, therefore, the gas seal is very expensive, and its repair is not cheap [Blasiak 2018 & 2022, Nagoev 2021].

This article proposes to consider a promising design of a gas seal with a impulse principle of creating and maintaining contactless operation – a gas barrier impulse face seal (GbIFS). In this seal, there is no difficult-to-manufacture gas-dynamic relief on the working face surfaces of the sealing rings, but the seal works stably in a wide range of pressures and temperatures of the pumped product, rotational speeds of the centrifugal pump rotor, and the performance characteristics are very similar to those of gas-dynamic seals with microrelief. At the same time, unlike gas-dynamic seals, this GbIFS design is more compact and has fewer parts, since it uses not two, but only one pair of face sealing rings. The size of the working gap between these sealing rings is set and maintained automatically, but also can be forcibly changed by changing the barrier gas supply pressure (Fig. 1).

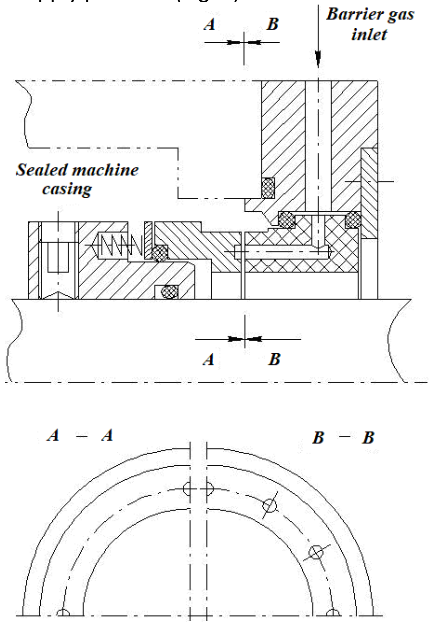

Figure 1. The design of the gas barrier-impulse face seal

The seal functions as follows. The barrier gas under pressure p_1 is supplied into the working gap of the seal through the orifices on the face surface of the sealing ring fixed in the housing (through the feeders). In parking mode, when the rotor shaft is not rotating, the pressure exerted by the feeders is insufficient to push apart the sealing rings, which are tightly together by springs and the pressure of the pumped product p_3. The gas evenly fills the operation gap and prevents to leak the pumped product from the pump casing. When the shaft rotates, special pits (chambers) on the face surface of the rotating ring begin for a short time (for a time t) is aligned with the orifices of the feeders on the face surface of the fixed sealing ring. When the gas enters the chamber from the feeder, it begins to compress to a pressure value of $p_{2\max} = p_1$. After the chamber ceases to be aligned with the feeder (for a period of time $T-t$; the time between two consecutive complete alignments of the camera with the supply channel is T), the pressure of the gas accumulated in it begins to decrease smoothly due to its outflow into the operating gap. This creates an additional force that helps the gas pressure from the feeders to push the sealing rings apart. This creates an operation gap that allows the seal to operate in a non-contact mode. Since the rate of pressure drop in the chamber depends on the size of the operation gap between the sealing rings, the gap value x is automatically set to exactly the value at which the flow rate of the barrier gas flow rate through the operation gap takes the minimum value for a given combination of the barrier gas pressure, the pressure of the product pumped by the pump and the speed of rotation of the pump rotor ω. The rate of gas flow from the chambers and feeders into the gap depends on the radial length of the working gap. The larger it is, the higher the resistance of the gap to gas flowing through it. Also, the rate of gas outflow from the chamber and, as a result, the minimum value of gas pressure in the closed chamber $p_{2\min}$ is affected by the frequency of alignment of chambers with feeders. If the dimensions of the radial extent of the gap sections, the dimensions of the chambers and feeders, as well as the hydraulic load coefficient on the movable sealing ring are correctly assigned, then at the operating pressures of the pumped product and the barrier gas, the minimum pressure in each chamber $p_{2\min}$ remains higher than p_3, that is, leakage of the pumped product through the operation gap will not occur. If we take into account that the distance between the chambers in the circumferential direction is not large, then, to a first approximation, we can assume that the gas pressure in the gap at the radius of the holes of the chambers and feeders is on average equal $\bar{p}_2$, while $\bar{p}_2 > p_3$.

2 RESEARCH METHODOLOGY

Although the operation of the GbIFS can be fully described in one paragraph of the text, the seal design is a complex gas-dynamic system in which an automatically adjustable operation gap of only a few microns ensures stable non-contact operation of the seal even if the operating parameters inevitably deviate from the nominal values in real conditions. Therefore, when designing this seal, the main task is to find the sealing ring sizes that will ensure the full operability of the seal in a given range of rotor speeds, sealing and barrier pressures, and eliminate the possibility of the pumped product breaking through the operation gap [Li 2005, Roberts-Haritonov 2005, Thomas 2006].

When creating a mathematical model of the working process, the following assumptions are made:

• the gas flow in the end gap is isothermal, laminar, stable, subsonic, pressurized, radial, axisymmetric;

• the operation gap between the sealing face surfaces is flat;

• the pressure change in each chamber is linear;

• the inertial forces of the gas in the operation gap and the frictional forces in the secondary seal are negligible, so should be ignored.

When the seal is operating, a system of forces acts on the surfaces of the axially and circumferentially movable sealing ring [Zahorulko 2015]. Under the influence of these forces, the ring occupies a position in which the forces acting on the sealing ring from the side of the operation gap are balanced by the forces acting on the back of the ring. Since the rotation of the ring periodically aligns the chambers with the feeders, the force on the ring from the gap side changes cyclically and therefore the ring constantly shifts to one side or the other along the shaft axis. The equation describing this motion has the standard form:

$$m\ddot{x} + c\dot{x} + k(\Delta + x) = F_c + F_s \tag{1}$$

Here m is the mass of the ring; c – the coefficient of resistance to movement, equal to the dynamic viscosity of the gas μ with which the ring is in contact; k – the stiffness of the springs; Δ – the amount of pre–compression of the springs; F_c and F_s – the integral values of the forces acting on the ring (Fig. 2).

The values of the forces F_s and F_c are determined by pressure diagrams acting on the corresponding sections of the working and rear surfaces of the ring. The law of gas pressure distribution in radial directions from the area of chambers and feeders into the pump cavity and into the space behind the seal (usually the room in which the pump is installed) can be calculated by integrating the one–dimensional Reynolds's equation $\frac{\partial}{\partial r}\left(r x^3 \frac{\rho}{\mu}\frac{\partial p}{\partial r}\right) = 0$. Thus, we can write:

$$\begin{gathered} F_s = \frac{2}{3}\frac{(\bar{p}_2^3 - p_3^3)}{(\bar{p}_2^2 - p_3^2)} S_{23} + \bar{p}_2 S_{22} + \frac{2}{3}\frac{(\bar{p}_2^3 - p_4^3)}{(\bar{p}_2^2 - p_4^2)} S_{24} \\ F_c = p_3 S_{35} + p_4 S_{54} + F_p \end{gathered} \tag{2}$$

Here S_{ij} are the areas affected by pressure on the side of the operation gap and on the back of the ring; F_p – spring compression force, p_4 – pressure behind the seal.

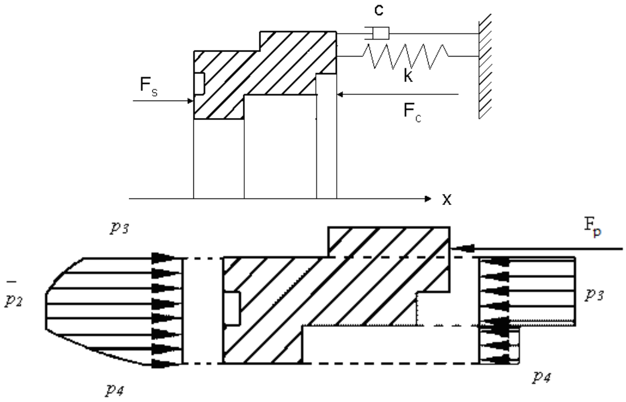

Figure 2. Scheme for calculating the seal characteristics

The distribution of gas flow rates from the chamber into the pump cavity and into the area behind the seal is determined by the expression (3):

$$\begin{aligned} & t\frac{2V_k}{RT^o}\frac{(p_1 - \bar{p}_2)}{t} = \\ & = (T-t)\frac{\alpha x^3}{24\mu R T^o \ln\left(\frac{r_3}{r_{23}}\right)}\left(\bar{p}_2^2 - p_3^2\right) + \\ & + (T-t)\frac{\alpha x^3}{24\mu R T^o \ln\left(\frac{r_{24}}{r_4}\right)}\left(\bar{p}_2^2 - p_4^2\right) + \\ & + \frac{\pi\left(r_3^2 - r_4^2\right)}{i}\dot{x} + \frac{V_k}{RT^0}\dot{\bar{p}}_2 \end{aligned} \tag{3}$$

Here V_k is the volume of each closed chamber; R is the gas constant for the barrier gas; T^0 is the absolute temperature of the barrier gas.

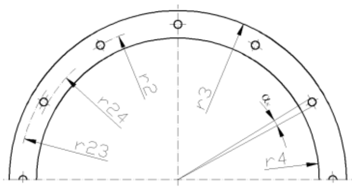

Figure 3. Geometric dimensions of the sealing ring

In a generalized form, this equation can be rewritten as follows (4):

$$t Q_{m12} = (T-t) Q_{m23} + (T-t) Q_{m24} + Q_{\Delta V} + Q_{\Delta p} \tag{4}$$

Here Q_{m12} is the mass flow rate of the compressing gas in a closed chamber during its flow from the feeder to the chamber; Q_{m23} – the mass flow rate of the barrier gas from the chamber into the pump casing; Q_{m24} – the mass flow rate of the barrier gas from the chamber to the area behind the seal; $Q_{\Delta V}$ – the flow rate of the displacing gas from the gap; $Q_{\Delta p}$ – the flow rate of the compressing gas in the chambers when the pressure changes caused by gap fluctuations [Kuznetsov 2023].

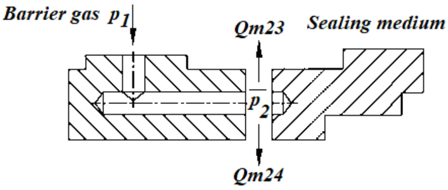

Figure 4. Gas flow diagram in a GbIFS

According to the calculation method [Kuznetsov 2024], this equation can be written in dimensionless form by the conductivity of the barrier gas flow channels, gas accumulation in the chambers and gas displacement from the gap:

$$q_{m12b}\,\Omega(\psi_1-\psi_2)=q_{m23b}\,u^3\left(\psi_2^2-\psi_3^2\right)+ +q_{m24b}\,u^3\left(\psi_2^2-\psi_4^2\right)+q_{m\Delta Vb}\cdot\dot{u}+q_{m\Delta pb}\cdot\dot{\psi}_2 \qquad (5)$$

Here $\psi_1=p_1/p_b$, $\psi_2=\bar{p}_2/p_b$, $\psi_3=p_3/p_b$, $\psi_4=p_4/p_b$ are the dimensionless barrier gas supply pressure, the pressure in the chambers, the pressure of the pumped product in the pump casing and the pressure behind the seal, respectively; $u=x/x_b$ – the dimensionless size of the operation gap; $\Omega=\omega/\omega_b$ – the dimensionless angular speed of the pump rotor. The values with the index are the values of the nominal operating mode of the seal.

The equation of the equilibrium position of the axially movable sealing ring can also be written in dimensionless form using (2):

$$\frac{2}{3}\frac{\psi_2^3-\psi_3^3}{\psi_2^2-\psi_3^2}\frac{S_{23}}{S_b}+\psi_2\frac{S_{22}}{S_b}+\frac{2}{3}\frac{\psi_2^3-\psi_4^3}{\psi_2^2-\psi_4^2}\frac{S_{24}}{S_b}= =\psi_3\frac{S_{35}}{S_b}+\psi_4\frac{S_{54}}{S_b}+\lambda \qquad (6)$$

Here $\lambda=F_p/S_b p_b$ is the immeasurable pre-compression force of the springs.

Solving equations (5) and (6) together, we obtain a complete mathematical model of the GbIFS working process. If we linearize the dependencies of this model in the static equilibrium position and present the result in an abbreviated form using the time differentiation operator $p=d/dt$, then we can write:

$$(T_1p+1)\psi_2=-k_\psi(T_2p+1)u+ +C_1\psi_1+C_3\psi_3+C_4\psi_4+C_0\Omega \qquad (7)$$

Hereafter, T_i, C_i, k_ψ are the time and geometric constants obtained after linearization, depending on the steady–state values of ψ_{10}, ψ_{20}, ψ_{30}, ψ_{40} as well as u_0 and Ω_0.

From (7) the dynamic rigidity of the system is easily determined:

$$\Phi(p)=-k_\psi\frac{T_2p+1}{T_1p+1} \qquad (8)$$

For harmonically varying processes $p=i\omega$, therefore, the frequency transfer function of the regulator:

$$\Phi(i\omega)=-\frac{\left(T_1T_2\omega^2+1\right)k_\psi}{T_1^2\omega+1}+i\omega\frac{T_1-k_\psi T_2}{T_1^2\omega+1} \qquad (9)$$

Here, the first term represents the elastic component, and the second one represents the damping component.

The equation of the dynamics of the system:

$$D(p)u=\left(a_3p^3+a_2p^2+a_1p+a_0\right)u= =Y_2(T_1p+1)\psi_1+Y_3(T_1p+1)\psi_4+ +C_1Y_1\psi_1+C_3Y_1\psi_3+C_4Y_1\psi_4+C_0Y_1\Omega \qquad (10)$$

Here $a_3=T_3^2T_1$, $a_2=T_3^2+T_1T_4$, $a_1=T_4+\lambda T_1+T_2k$, $a_0=\lambda+k_\psi$, Y_i are the geometric constants obtained after linearization.

The analysis of the dynamic system makes it possible to determine the condition of its stability:

$$T_2>\frac{(-\lambda T_4)T_1^2+\left(k_\psi T_3^2-T_4^2\right)T_1-\left(T_3^2T_4\right)}{\left(T_4k_\psi\right)T_1+\left(k_\psi T_3^2\right)} \qquad (11)$$

Frequency transfer functions of seal by external influences ψ_1, ψ_3, ψ_4 and Ω:

$$\Phi_{\psi1}=\frac{u}{\psi_1}=\frac{C_1Y_1}{D(i\omega)}$$

$$\Phi_{\psi3}=\frac{u}{\psi_3}=\frac{\left(b_{1\psi3}\right)p+\left(b_{0\psi3}\right)}{D(i\omega)}$$

$$\Phi_{\psi4}=\frac{u}{\psi_4}=\frac{\left(b_{1\psi4}\right)p+\left(b_{0\psi4}\right)}{D(i\omega)} \qquad (12)$$

$$\Phi_\Omega=\frac{u}{\Omega}=\frac{C_0Y_1}{D(i\omega)}$$

Here $b_{i\psi j}=Y_jT_i$, $b_{0\psi j}=C_jY_i-Y_j$.

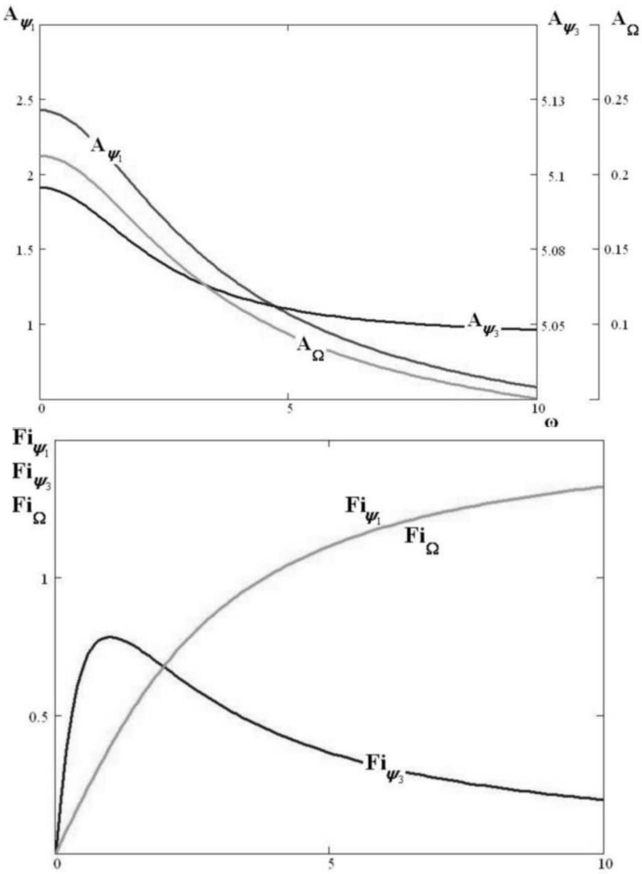

Figure 5. Amplitude and phase frequency characteristics of the GbIFS

The amplitude and phase frequency characteristics are written as (5):

$$A_{\psi i,\Omega} = \frac{C_{i,0}Y_i}{\sqrt{L^2 + M^2}}$$

$$A_{\psi i,\psi j} = \sqrt{\frac{b_{0\psi i,0\psi j}^2 + \omega^2 b_{1\psi i,1\psi j}^2}{L^2 + M^2}} \qquad (13)$$

$$Fi_{\psi 1,\Omega} = arctg\frac{M}{L}$$

$$Fi_{\psi i,\psi j} = arctg\frac{L\omega b_{1\psi i,1\psi j} + M b_{0\psi i,0\psi j}}{L b_{0\psi i,0\psi j} + M\omega b_{1\psi i,1\psi j}}$$

Here: $L = a_0 - a_2\omega^2$, $M = a_1\omega - a_3\omega^3$.

These dependencies make it possible to determine the response of the movable ring to input harmonic changes in external influences, identify dangerous frequency values regions, and select sealing parameters at which the oscillation amplitudes of the movable ring do not exceed the permissible limits.

3 CONCLUSIONS

The mathematical model of the GbIFS working process presented in this article is based on a standard approach to calculating non-contact impulse liquid seals, which assumes that the pressure in a closed chamber and the pressure in the gap between the chambers differ little from each other. This leads to the fact that the model assumes that to determine the pressure $\overline{p}_2$, it is sufficient to consider only the distribution of gas flow through a single chamber, and the same pressure value will act in the entire circular area of the operation gap where the openings of the chambers and feeders are located. From the authors' point of view, this simplification is acceptable if the distance between adjacent cameras is significantly less than the length of the cameras themselves. The actual effect of the operation gap section between the chambers on the nature of the pressure distribution of the barrier gas can be estimated only by numerically solving the problem of pressure distribution in the gap [Kuznetsov 2020]. Experimental studies of gas barrier impulse face seals have shown that by varying the number of chambers, it is possible to achieve a significant change in the sealing performance. Moreover, not only their quantitative, but also their qualitative indicators are changing [Kuznetsov 2019].

ACKNOWLEDGMENTS

The authors would like to thank the KEGA grant agency for supporting research work and financing the project KEGA 008TUKE-4/2025.

REFERENCES

[Blasiak 2018] Blasiak, S. Numerical modeling and analysis of the noncontacting impulse gas face seals. Proceedings of the Institution of Mechanical Engineers, Part J: Journal of Engineering Tribology, 2018, Vol. 233, No. 8, pp. 1139-1153. DOI: 10.1177/1350650118817188.

[Blasiak 2022] Blasiak, S. and Takosoglu, J. Analysis of Pressure Distribution in Non-Contacting Impulse Gas Face Seals. Materials Research Proceedings, 2022, Vol. 24, pp. 254-261. DOI: https://doi.org/10.21741/9781644902059-37.

[Brunetiere 2024] Brunetiere, N., Zahorulko, A., Bouyer, J. Numerical Simulation of the Behavior of Impulse Gas Seals. Tribology Online, 2024, Vol. 19, Issue 4, pp. 360-366. https://doi.org/10.2474/trol.19.360.

[Kuznetsov 2019] Kuznetsov, E., Panda, A., Nahornyi, V., et al. Experimental Researches of the Pulse Gas barrier Face Seal. MM Science Journal, 2019, No. December, pp. 3519-3523. DOI: 10.17973/MMSJ.2019_12_2019033.

[Kuznetsov 2020] Kuznetsov E., Nahornyi V., Krenicky T. Gas Flow Simulation in the Working Gap of Impulse Gas-Barrier Face Seal. Management Systems in Production Engineering, 2020, Vol. 28, Issue 4, pp. 298-303. DOI: 10.2478/mspe-2020-0042.

[Kuznetsov 2023] Kuznetsov, E., Pandova, I. Calculation of the Operational Characteristics of the Impulse Gas-Barrier Face Seal. Management Systems in Production Engineering, 2023, Vol. 31, Issue 4, pp. 411-417. DOI: 10.2478/mspe-2023-0046.

[Kuznetsov 2024] Kuznetsov, E., Panda, A., Nahornyi, V. Calculation of Dynamic Characteristics of a Face Gas-Barrier Impulse Seal for Pump and Compressor Shafts. MM Science J., 2024, No. October, pp. 7442-7446. DOI: 10.17973/MMSJ.2024_10_2024004.

[Li 2005] Li, J. Mathematical Simulation of Flow in Gas Face Seals. Journal of Sichuan University, 2005. Available from: http://en.cnki.com.cn/Article_en/CJFDTOTAL-SCLH200503030.htm

[Martsynkovskyy 2014] Martsynkovskyy, V., Kundera, C., Khalizeva, A. The Calculation of Static Characteristics of Impulse Gas Seal. Applied Mechanics and Materials, 2014, Vol. 630, pp. 267-276. 10.4028/www.scientific.net/AMM.630.267.

[Nagoev 2021] Nagoev, Z., Narozhnov, V., Pskhu, A., Rekhviashvili, S. Protective Face Shield Effectiveness: Mathematical Modelling. Springer: Singapore, 2021, pp. 35-50. https://doi.org/10.1007/978-981-16-2450-6_3.

[Panda 2021] Panda, A., Anisimov, Volodymyr, et al. Increasing of wear resistance of linear block-polyurethanes by thermal processing methods. MM Science Journal, 2021, No. October, pp. 4731-4735.

[Sukhodub 2019] Sukhodub, L., Panda, A., Sukhodub, L., Kumeda, M., Baron, P. Hydroxyapatite and zinc oxide based two-layer coating, deposited on Ti6Al4V substrate. MM Science Journal, 2019, No. December, pp. 3494-3499.

[Thomas 2006] Thomas, S., Brunetiere, N., Tournerie, B. Numerical Modelling of High Pressure Gas Face Seals. Journal of Tribology-Transactions of The Asme, 2006, Vol. 128, No. 2, pp. 396-405. https://doi.org/10.1115/1.2164471.

[Roberts-Haritonov 2005] Roberts-Haritonov, L. and Reed, J. Gas seal assembly. 2005. Available from: https://patents.google.com/patent/US2007022216 0A1/en.

[Zaborowski 2007] Zaborowski, T. Ekowytwarzanie. Gorzow, 2007, 100 p.

[Zahorulko 2015] Zahorulko, A.V. Theoretical and experimental investigations of face buffer impulse seals with discrete supplying. Eastern-European Journal of Enterprise Technologies, 2015, Vol. 4, No. 7, pp. 45-52. DOI: https://doi.org/10.15587/1729-4061.2015.48298.

CONTACTS:

Anton Panda, Prof. Eng. PhD.
Faculty of Manufacturing Technologies with a seat in Presov
Technical University of Kosice
Sturova 31, 080 001 Presov, Slovakia
e-mail: anton.panda@tuke.sk